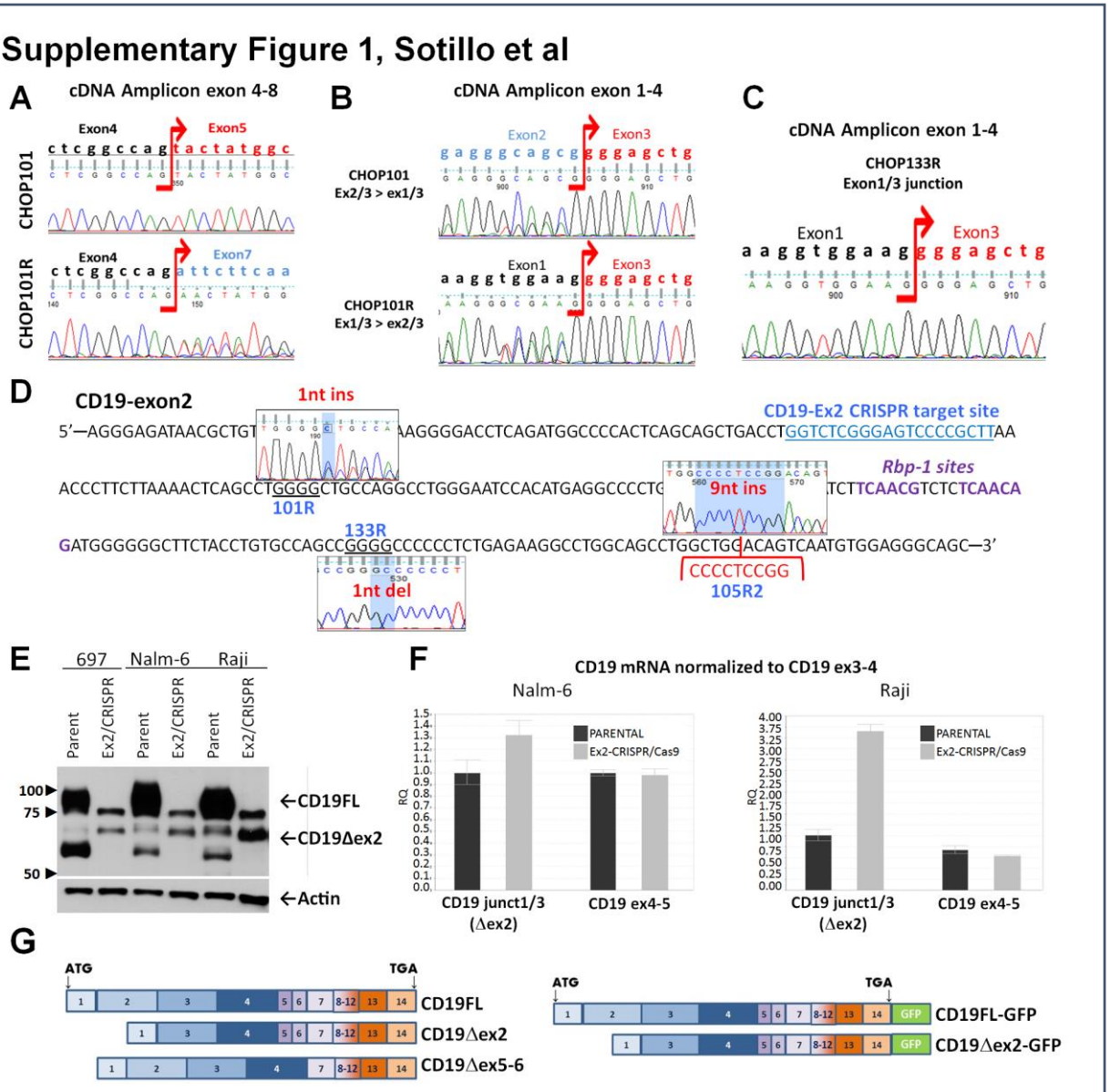

Figure S1. Enhanced skipping of exons 2 and 5-6 in post-CART-19 leukemias. a, Detail from Sanger sequencing of exon4-8 cDNA obtained from xenografted samples showing enhanced skipping of exons 5 and 6 in the relapse CHOP101R sample. **b,** Detail of Sanger sequencing of the exon 1-4 cDNA showing Exon2/3junction. Major traces align with exon2-exon3 in CHOP101 (top), while exon 1-exon3 junction dominates in sample CHOP101R (bottom). **c,** Detail of Sanger sequencing of the exon1-4 cDNA from sample CHOP133R showing that only exon1-3 junction is detectable. This sample has a hemizygous deletion of Chromosome 16 and the remaining CD19 allele carries a nonsense mutation in exon 2. **d,** Summary of mutations found in post-CART19 relapsed leukemias along CD19 exon 2. Highlighted in blue is the CRISPR/Cas9 targeted sequence used to introduce mutations in exon2. Highlighted in purple are predicted binding sites for Rbp-1, the Drosophila homologue of SRSF3. **e,** Immunoblotting for CD19 in protein lysates from a panel of human lymphoid B cell lines that were targeted with CRISPR/Cas9-CD19exon2-gRNA. Arrows indicate full length (FL) and the Δex2 isoform. The antibody used (Cell signaling) recognizes the cytosolic domain. **f,** qRT-PCR analysis of CD19 splicing variants in Nalm-6 (left) and Raji (right) cells targeted with CRISPR/Cas9 as in panel e. Oligos used span *conserved* and alternative exon/exon junctions. Graph shows relative quantification of expression ± 1 .S.D. Oligos expanding exon3/4 of CD19 were used as reference. **g,** Retroviral constructs generated to ectopically express full-length and truncated isoforms of CD19, with or without GFP.

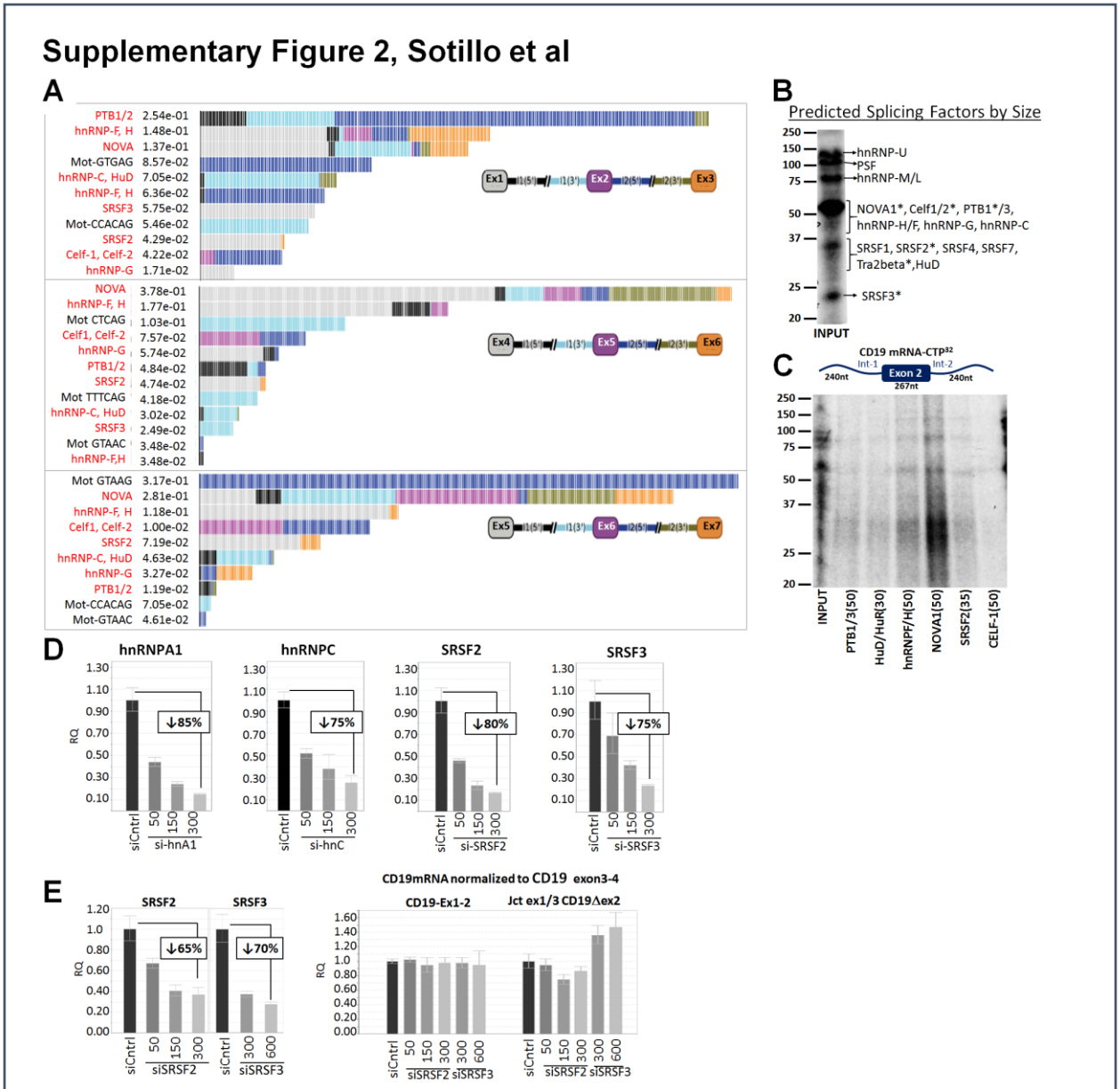

Figure S2. Analysis of splicing factors involved in alternative splicing of CD19-exon2. a, Splicing factors predicted by the AVISPA algorithm to process introns 1 and 2 and introns 4, 5, and 6 of the CD19 mRNA. Numbers represent the predicted normalized feature effect (NFE) score, colors represent contribution of the binding motifs in the matching regions. Highlighted in red are those factors that overlap in all three analyzed cassettes **b,** RNA pull-down assay for detection of splicing factors present in nuclear extracts of B cells that bind to CD19-exon2 and its flanking introns. Input lane shows pattern of bands corresponding to all nuclear proteins that bind the CD19-minigene. Putative splicing factors with molecular sizes similar to the bands detected are listed. (*) Indicates those that were also predicted by AVISPA. **c,** RNA-immunoprecipitations were performed using antibodies against indicated proteins. Numbers in parentheses indicated expected molecular weights for each protein. **d,** Efficiency of siRNA knock-down in P493-6 cells transfected with increasing concentrations of indicated siRNAs for 24h, as measured by qRT-PCR. **e, left:** Efficiency of siRNA knock-down in Nalm-6 cells transfected with increasing concentrations of indicated siRNAs for 24h. **right:** qRT-PCR analysis of CD19 Δex2 splicing variant in the same samples.